Cobaltocenium-Functionalized Poly(propylene imine) Dendrimers: Redox and Electromicrogravimetric Studies and AFM Imaging

Kazutake Takada,[b] Diego J. Díaz,[b] Héctor D. Abruña,*[b] Isabel Cuadrado,*[a] Blanca González,[a] Carmen M. Casado,[a] Beatriz Alonso,[a] Moisés Morán,[a] and José Losada[c]

Abstract: The first four generations of cobaltocenium-functionalized, diaminobutane-based poly(propylene imine) dendrimers DAB-*dend*-$Cb_x(PF_6)_x$ ($x =$ 4, 8, 16, and 32; Cb = {Co(η^5-C_5H_4CONH)(η^5-C_5H_5)} (**1**–**4**) have been synthesized and characterized. The redox activity of the cobaltocenium centers in **1**–**4** has been characterized by using cyclic voltammetry and the electrochemical quartz-crystal microbalance (EQCM). All of the dendrimers exhibit reversible redox chemistry associated with the cobaltocenium/cobaltocene redox couple. Upon reduction, the dendrimers exhibit a tendency to electrodeposit onto the electrode surface, which is more pronounced for the higher generations. Pt and glassy carbon electrodes could be modified with films derived from **1**–**4**,exhibiting a well-defined and persistent electrochemical response. EQCM measurements show that the dendrimers adsorb, at open circuit, onto platinum surfaces at monolayer or submonolayer coverage. Cathodic potential scanning past -0.75 V at which the cobaltocenium sites are reduced, gave rise to the electrodeposition of multilayer equivalents of the dendrimers. The additional material gradually desorbs upon re-oxidation so that only a monolayer equivalent remains on the electrode surface. Changes in film morphology as a function of dendrimer generation and surface coverage were studied by using admittance measurements of the quartz-crystal resonator on the basis of its electrical equivalent circuit, especially in terms of its resistance parameter. In general, we find that films of the lower dendrimer generation **1** behave rigidly, whereas those of the higher generation **4** exhibit viscoelastic behavior with an intermediate behavior being exhibited by **2** and **3**. Using tapping-mode atomic force microscopy (AFM), we have been able to obtain molecularly resolved images of dendrimer **4** adsorbed on a Pt(111) electrode.

Keywords: dendrimers · electrochemistry · metallocenes · quartz-crystal microbalance

Introduction

The synthesis of dendrimers, highly branched polymers of well-defined architecture, has expanded very rapidly in the last decade.[1] These materials are attracting considerable attention in many different areas of science and technology, owing to the range of promising applications and their new and unique architectural features; these include their precise constitution, well-defined internal cavities, nanometer dimensions, and the presence of a large number of functionalities on the surface. Likewise, the incorporation of metals within or on the periphery of dendritic structures is another exciting feature as it has provided access to new materials capable of novel magnetic, electronic, photophysical, or catalytic properties.[2–7]

In the context of organometallic dendrimers, ferrocene has been the most widely used redox-active moiety incorporated into dendritic structures. In this way, we and others have recently developed different synthetic routes to prepare ferrocenyl dendrimers of controlled nuclearity and chemical structure.[8–13] In such globally neutral dendrimers, the ferrocenyl moieties may behave independently in an overall multielectron processes, or on the other hand electronic communication may exist between ferrocenyl groups linked together in close proximity to one another.[9] We have employed these

[a] Dr. I. Cuadrado, B. González, Dr. C. M. Casado, Dr. B. Alonso, Prof. Dr. M. Morán
Departamento de Química Inórganica
Universidad Autónoma de Madrid,
Cantoblanco 28049, Madrid (Spain)
Fax: (34) 913-974833
E-mail: isabel.cuadrado@uam.es

[b] Prof. Dr. H. D. Abruña, Dr. K. Takada, Dr. D. J. Díaz
Department of Chemistry and Chemical Biology
Baker Laboratory, Cornell University, Ithaca
New York 14853-1301 (USA)
Fax: (01) 607-255-9864
E-mail: hda1@cornell.edu

[c] Dr. J. Losada
Escuela Técnica Superior de Ingenieros Industriales
Universidad Politécnica de Madrid, 28006 Madrid (Spain)

  0947-6539/01/0705-1109 $ 17.50+.50/0

dendritic polymetallocenes as novel materials for the modification of electrode surfaces,[14] as electrochemical biosensors,[15] as multisite guests for supramolecular assemblies,[16] and as sensors for anions.[17]

In contrast, to date very few examples of polycationic redox-active organometallic dendrimers have been prepared.[18] Cobaltocenium also constitutes an excellent organometallic moiety to incorporate in or functionalize dendritic systems as it is a highly stable, positively charged complex isoelectronic with ferrocene, and undergoes a reversible monoelectronic reduction to yield the neutral cobaltocene. With this in mind, we have recently prepared polycationic dendrimers based in poly(propylene imine) backbones, containing 4, 8, 16, and 32 cobaltocenium functional groups located at the periphery of the dendritic structures, and we have found that while the oxidized (Co^{III}) dendrimers do not interact with β-cyclodextrin hosts, multiple inclusion complexes are formed upon dendrimer reduction to the cobaltocene (Co^{II}) form.[19]

As a follow up to this earlier communication, we now report full details on the synthesis, characterization, and redox properties of this family of cobaltocenium dendrimers, along with the electrochemical behavior of electrodes modified with these metallodendrimers. In addition, we have carried out electrochemical quartz-crystal microbalance (EQCM) studies including impedance measurements (resistance parameter) of electrodes modified with electrodeposited films of these dendrimers. Moreover, we have also employed scanned probe microscopic techniques, with emphasis on atomic force microscopy, in an effort to ascertain the structure and topology of these electrodeposited dendritic materials. These studies could provide valuable insights not only toward the understanding of interfacial reactions but also toward the modification of electrodes for applications as multielectron-transfer mediators, catalysts, sensors, and electronic devices.

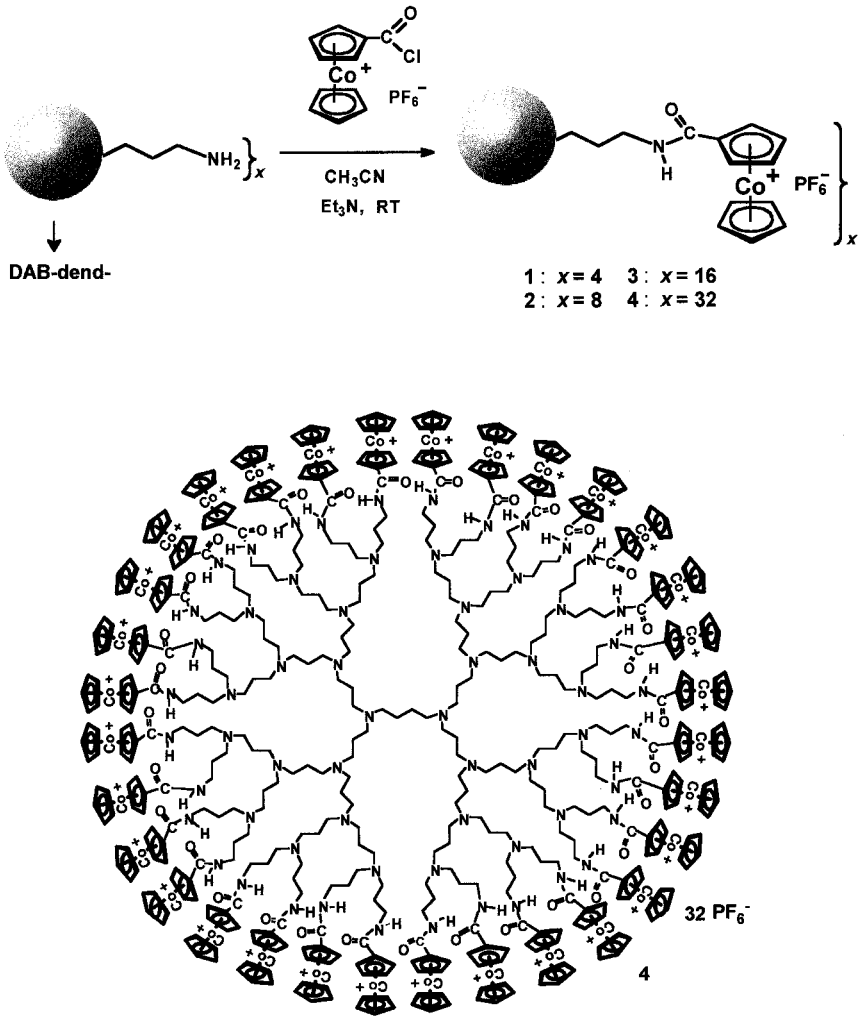

Scheme 1. Preparation of dendrimers **1**–**4**.

Results and Discussion

Syntheses and characterization of dendrimers: The cobaltocenium dendrimers DAB-*dend*-$Cb_x(PF_6)_x$ [$x = 4$, 8, 16, and 32; $Cb = \{Co(\eta^5\text{-}C_5H_4CONH)(\eta^5\text{-}C_5H_5)\}$] (**1**–**4**) have been obtained by treatment of the first four generations of diaminobutane-based poly(propylene imine) dendrimers (DAB-*dend*-$(NH_2)_x$, $x = 4$, 8, 16, and 32) with an excess of the PF_6^- salt of 1-(chlorocarbonyl)cobaltocenium in CH_3CN solution (Scheme 1). Purification was carried out by dissolution in CH_3CN and precipitation with dichloromethane followed by column chromatography with CH_3CN as eluent. Dendrimers **1**–**4** were isolated as air-stable yellow to greenish shiny solids, soluble in solvents such as CH_3CN, DMSO, DMF, and acetone and insoluble in CH_2Cl_2.

The structural identities of the polycationic metallodendrimers were confirmed by ^1H, ^{13}C NMR, and IR spectroscopy, electrospray ionization mass spectrometry (ESI-MS), and fast atom bombardment mass spectrometry (FAB-MS). The ^1H NMR spectra of **1**–**4** show the signals of the poly(propylene imine) dendritic framework and the key signals arising from the cobaltocenium fragments, which are observed in the range $\delta = 5.8$–6.4. The completion of the condensation reaction was indicated by the total absence, in the ^1H NMR spectra, of the NH_2 signals of the starting dendritic polyamines around $\delta = 1.3$, as well as by the

0947-6539/01/0705-1110 $ 17.50+.50/0 *Chem. Eur. J.* **2001**, *7*, No. 5

appearance of a new signal in the range $\delta = 8.2 - 9.1$ due to the amide group, and the downfield shift (from $\delta = 2.6$ to $3.3 - 3.5$) of the resonance corresponding to the adjacent methylene. In addition, the complete amidation was further supported by the integration ratios of the different protons, which are in agreement with the expected structures. The structures of the polycationic dendrimers were corroborated by FAB-MS for the first- and second-generation dendrimers **1** and **2**, and by ESI-MS for **3**. In all cases, the mass spectra show different peaks corresponding to species with different states of charge, which result from the successive loss of counteranions. Thus, for example for dendrimer **3** peaks at *m/z* 1096, 919, 786, 683, 600, 532, and 476 can be assigned to the loss of from 6 to 12 PF_6^- counteranions, respectively. Surprisingly, under the same experimental conditions, ESI-MS mass spectrometric technique failed to give a useful spectrum of dendrimer **4**. Appropriate conditions to register clear ESI-MS or MALDI-TOF spectra with good signals to noise ratios have not yet been obtained.

Cyclic voltammetric studies: The electrochemical behavior of the synthesized cobaltocenium dendrimers **1**–**4** has been investigated by cyclic voltammetry (CV) of the materials in homogenous solution, as well as that confined to electrode surfaces (i.e., where the dendrimers serve as electrode modifiers). For all generations (**1**–**4**) of this dendritic family that we have studied, a single redox process is observed in CH_3CN with a formal potential (E°) of about -0.72 V versus SCE (Table 1); a value that is about 200 mV more positive than that exhibited by cobaltocenium in the same medium (vide infra). Thus, the aforementioned wave is ascribed to the simultaneous one-electron reduction of all the peripheral cobaltocenium moieties at the same potential. In addition, a second and irreversible redox process, corresponding to the reduction of the multiple cobaltocene centers, is observed at about -1.70 V.

Table 1. Electrochemical parameters for dendrimers **1**–**4**.

	$E^{o\prime}$ [V] versus SCE	D_{oNPV} [$cm^2 s^{-1}$]	D_{oCV} [$cm^2 s^{-1}$]
1	-0.73	9.63×10^{-6}	1.95×10^{-6}
2	-0.72	3.56×10^{-6}	6.49×10^{-6}
3	-0.72	3.18×10^{-6}	2.28×10^{-7}
4	-0.72	3.00×10^{-6}	2.19×10^{-7}
$[(\eta^5\text{-}C_5H_5)_2Co]PF_6$	-0.92	1.51×10^{-5}	2.16×10^{-5}

It is worth noting that the solution redox behavior is sensitive to the dendrimer generation. In order to check the evolution of this dendritic effect on the voltammetric response, cyclic voltammograms of solutions of these polymetallic species in CH_3CN, containing the same molar amount of cobaltocenium units in all cases, were obtained (Figure 1). For the tetrametallic dendrimer **1** (Figure 1), reduction and oxidation (around the wave centered at -0.73 V) did not appear to affect the solubility of the dendrimer, so that the voltammetric response exhibited the wave shape characteristic of a freely diffusing soluble species undergoing reversible charge transfer. Consistent with this was the fact that the peak current scaled with the square root of the sweep rate as anticipated.

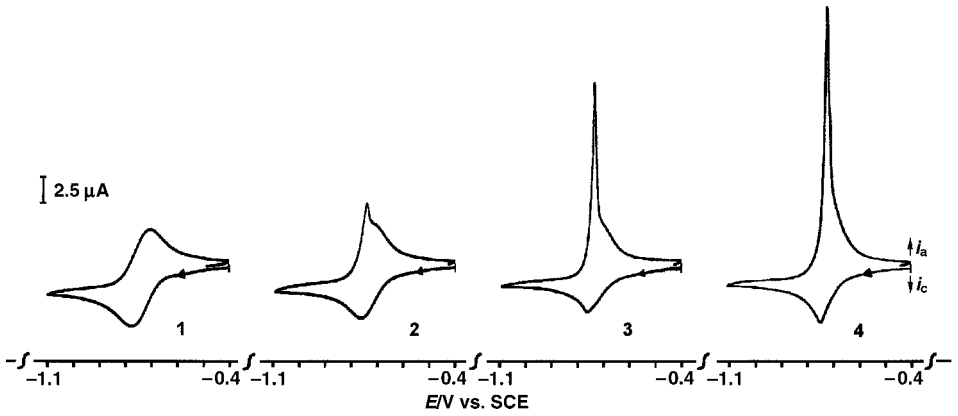

Figure 1. Cyclic voltammograms of the cobaltocenium dendrimers **1**, **2**, **3**, and **4** in CH_3CN/TBAH at 100 $mV s^{-1}$. The concentration of cobaltocenium centers is the same (1 mM) in each case.

On the other hand, for dendrimers of higher generations **2**–**4**, which contain 8, 16, and 32 cobaltocenium units, respectively, oxidation-state-dependent solubility changes were readily apparent. Thus, electroreduction of the cationic cobaltocenium dendrimers resulted in the deposition of the electrogenerated neutral cobaltocene dendrimers on the electrode surface. On the subsequent oxidative scan, the electrodeposited material was stripped upon oxidation. However, not all the deposited material was stripped from the surface in a single scan; this suggests that there might be some strong adsorbed dendrimer remaining on the electrode surface upon oxidation. Moreover, as the number of peripheral amide-linked cobaltocenium moieties per dendritic molecule increased (i.e., as the generation increased), the anodic stripping wave increased in magnitude (Figure 1). This behavior contrasts and is opposite to that previously observed for the analogous neutral ferrocenyl dendrimers DAB-*dend*-Fc_x ($x = 8$, 16, 32, or 64), which become insoluble upon oxidation to the corresponding polycationic macromolecules yielding dendrimer films on the electrode surface and which are stripped on the subsequent cathodic scan.[8c, 14b]

Because of the deposition of the neutral dendrimers **2**–**4** on the electrode surface, the formal potential values (E^o) for these reduction processes were determined by using normal pulse voltammetry (NPV), and the results are presented in Table 1. As alluded to above, the reduction of the cobaltocenium-functionalized dendrimers **1**–**4** occurs at a potential that is about 200 mV less negative than the corresponding process for $[(\eta^5\text{-}C_5H_5)_2Co]PF_6$ (-0.94 V versus SCE in CH_3CN). This is due to the strong electron-withdrawing

effect of the amide groups when bound directly to the metallocene units, making the reduction of the cobaltocenium dendrimers thermodynamically easier than that of unsubstituted cobaltocenium.

The diffusion coefficients, D_o, upon reduction for the four cobaltocenium dendrimers in CH_3CN have been calculated from CV and NPV[20] (by using the Cottrell equation), and the results are also presented in Table 1. As anticipated, the diffusion coefficients of dendritic molecules are lower than that of an organometallic monomer of small size such as cobaltocenium. It is also clear from Table 1 that the values of the diffusion coefficients obtained by NPV are not only about an order of magnitude larger than those obtained by CV, but also unrealistically high in some cases such as **4**. Although the use of NPV has been previously recommended for the measurement of diffusion coefficients of materials that adsorb,[21] in our case the very nature of the experiment gives rise to the anomalous results alluded to above. This arises, at least in part, because in NPV the time delay between pulses is too short to allow for material that has adsorbed on the forward pulse to desorb. Such an adsorbed layer would give rise to anomalously high currents, which in turn would result in high values of the diffusion coefficients. Diffusion coefficient measurements by CV would also be susceptible to the presence of an adsorbed layer of dendrimer, which, as we mentioned previously, we know to be present on the electrode surface prior to electroreduction of the cobaltocenium centers. However, the effect is compounded in the case of NPV because there are repeated excursions to potentials at which the cobaltocenium centers are reduced and, therefore, electrodeposited; this gives rise to the continued accumulation of material on the electrode. This is not the case for CV and, thus, we feel that diffusion coefficients measured by CV are more reliable in this particular instance. However, for the reasons mentioned above, these values must still be considered as somewhat elevated.

Turning to the specific values of the diffusion coefficients (obtained by CV), we note that, as a trend, the values decrease as the generation increases. However, values for **2** and **3** are virtually the same, which would suggest that they are of comparable size. It should be mentioned that these values are comparable to those for the analogous ferrocene derivatized dendrimers as well as for dendrimers containing $[Ru(tpy)_2]^{+2}$ centers (tpy = terpyridine). In the latter case we have also measured the diffusion coefficients using pulse field gradient spin-echo NMR spectroscopy and the values are generally in accordance.[22] Thus, as a general trend, as anticipated, the diffusion coefficient decreases with increasing generation.

A valuable feature of these organometallic dendrimers is their ability to modify electrodes, resulting in electroactive material that remains persistently attached to the electrode surface. The deposition of the dendrimers can be carried out onto Pt or glassy carbon electrodes, and presumably other materials, either by controlled potential electrolysis at -1.10 V or by repeated cycling between 0 and -1.10 V versus SCE in degassed solutions of dendrimer in CH_3CN. Thus, the amount of electrodeposited material can be controlled through the time interval, during which the potential or the number of scans was held fixed. As a representative example, Figure 2 shows the voltammetric response in aqueous solution of a Pt electrode modified with an electrodeposited film of dendrimer **3**, for which a well-defined, reversible wave is

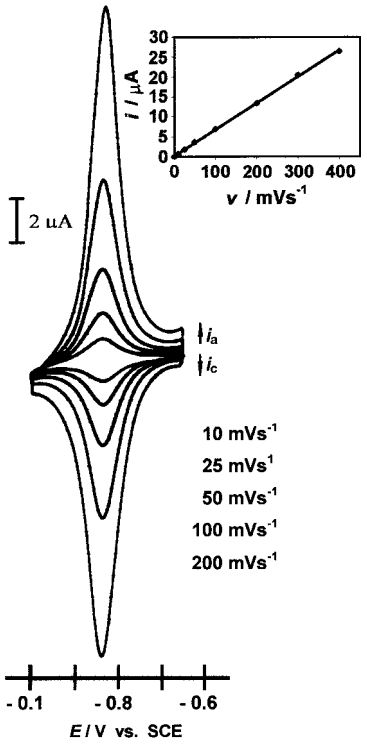

Figure 2. Cyclic voltammograms of a platinum-disk electrode modified with a film of dendrimer **3** measured in $H_2O/LiClO_4$. Inset: plot of peak current versus sweep rate.

observed at a formal potential value of -0.81 V corresponding to the cobaltocenium/cobaltocene couple. Qualitatively similar responses were obtained for modified glassy carbon electrodes.

The voltammetric wave-shape is that anticipated for a surface-confined redox reagent.[23] The current was linearly proportional to the sweep rate for values up to 500 mV s^{-1} (see inset in Figure 2), and peak potential difference (ΔE_p) values were typically small; these were about 10 mV at 200 mV s^{-1} and for sweep rates below 20 mV s^{-1} the splitting was virtually zero. However, for higher sweep rates, ΔE_p values tended to increase (e.g., ΔE_p was 20 mV at a sweep rate of 500 mV s^{-1}). These observations indicate that for sweep rates below about 500 mV s^{-1} these films exhibit rapid electron and charge-transfer kinetics. Extended potential cycling (e.g., 1 h at 100 mV s^{-1}) resulted in only a small loss ($<15\%$) of electrodeposited material and the voltammetric waveshape remained virtually unchanged; this demonstrates that electrodeposited films of **3** are stable to extended electrochemical cycling. This is an important observation since many of the anticipated applications will require extensive redox cycling.

From the integration of the area under the voltammetric wave (i.e., the charge) for the voltammogram presented in Figure 2, the surface coverage (of cobaltocenium sites) of **3** was estimated to be about 1.2×10^{-9} mol cm^{-2} (mol of

0947-6539/01/0705-1112 $ 17.50+.50/0 *Chem. Eur. J.* **2001**, *7*, No. 5

cobaltocenium sites cm^{-2}). This represents approximately two equivalent monolayers of immobilized cobaltocenium. By controlling the deposition conditions as described above, the coverage could be deliberately controlled from less than a monolayer to tens (e.g., 30) of monolayer equivalents. The fact that the waveshape anticipated for a surface-immobilized redox couple was maintained even at high surface-coverage values again confirms the fact that these systems exhibit rapid charge-transfer kinetics as stated above.

Electrochemical quartz-crystal microbalance (EQCM) studies: We have carried out EQCM and impedance studies, particularly with regards to the resistance parameter and its changes, of the electrodeposition processes of the cobaltocenium-containing dendrimers. Changes in mass during the electrodeposition of the dendrimers were monitored by changes in the frequency of an EQCM, while scanning the applied potential. In these experiments, a 0.2 mM solution concentration of cobaltocenium sites was used, which corresponded to 50, 25, 13, and 6.3 μM solutions for the dendrimers **1**, **2**, **3**, and **4**, respectively.

Figure 3 shows the typical cyclic voltammogram (A) and frequency responses (B) as a function of the applied potential for a Pt electrode on a quartz-crystal resonator in contact with

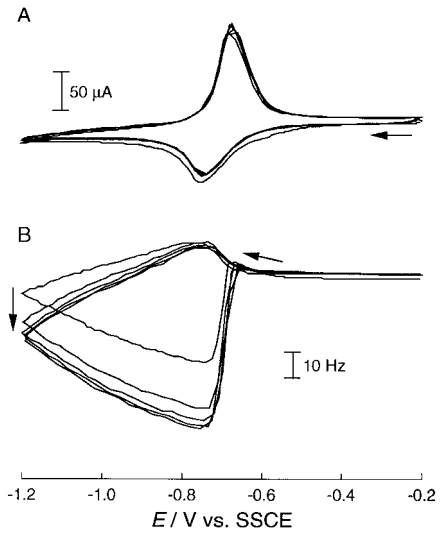

Figure 3. Typical A) current (CV) and B) frequency responses as a function of applied potential at 50 $mV s^{-1}$ for a Pt EQCM electrode in contact with a solution of dendrimer **4** (6.3 μM; 0.2 mM cobaltocenium sites).

a 0.10 M TBAH/CH_3CN solution containing 6.3 μM of dendrimer **4**. As was alluded to previously, cathodic waves showed primarily a diffusional shape, whereas anodic waves showed a typical stripping shape, an indication that the dendrimers adsorb onto the electrode during reduction and desorb during oxidation. The frequency responses obtained concurrently with the cyclic voltammograms also support these observations. Although there was a slight initial increase (vide-infra) the frequency largely decreased during the cathodic scan from about −0.75 V versus SSCE, which is just prior to the cathodic peak potential, to −1.20 V at which the sweep direction was reversed (Figure 3B). The frequency continued to decrease during the anodic scan up to −0.70 V, and then it increased sharply. The decrease in frequency (due mainly to a mass increase) upon reduction indicates the accumulation of the neutral dendrimer on the electrode surface. On the other hand, the sharp increase in the frequency (due mainly to a mass decrease) upon oxidation of the dendrimer to a +1 charge (per redox site) may be a manifestation of redissolution (stripping) of the previously deposited dendrimer. Although a strict comparison with the analogous ferrocenyl-containing dendrimers DAB-*dend*-Fc_x ($x = 8$, 16, 32, or 64)[14b] is difficult since the solvent and supporting electrolyte used in this work (TBAH/CH_3CN) were different from those used for the ferrocenyl dendrimers studies (TBAP/CH_2Cl_2, in which **4** is insoluble), these redox-state dependent deposition and desorption processes are opposite to those of the ferrocenyl dendrimers, in which the dendrimer accumulated upon oxidation and was desorbed/stripped in the subsequent reduction process.

The small increase in frequency (ca. 10 Hz) in Figure 3B just prior to the large decrease upon reduction might be caused by a release of anions to maintain charge neutrality in the deposited dendrimer film. On the other hand, the small decrease in the frequency just after the drastic increase in frequency upon oxidation might be assigned to the incorporation of anions. For these processes to occur, an adsorbed or deposited layer of the dendrimer must have been present on the electrode surface just upon contact of the electrode with the dendrimer solution. If, after coming into contact with the dendrimer solution (i.e., no applied potential) the electrode is transferred to a fresh TBAH/CH_2Cl_2 solution containing no dendrimer, a small peak corresponding to the reduction of the cobaltocenium centers was observed on the first cathodic potential scan. However, only a very small peak was observed in the reverse scan, and both peaks (cathodic and anodic) rapidly decayed upon further potential cycling. This indicates that the dendrimer adsorbs onto a Pt electrode at least in the presence of the dendrimer in the solution, in a manner analogous to DAB-*dend*-Fc_x[14b] and polyamidoamine dendrimers surface-functionalized with polypyridyl metal complexes.[24] If the 10 Hz increase in frequency alluded to above were due solely to anion ejection, this would correspond to a surface coverage of about 1.2×10^{-9} mol cm^{-2}, which is approximately two monolayer equivalents of cobaltocenium. A similar value is obtained from the first reductive sweep for an electrode placed in only supporting electrolyte after having been exposed to a solution of the dendrimer.

The anion-exchange behavior of the deposited films was better defined for the lower generation dendrimers, since changes in the frequency due to the deposition and desorption of the dendrimers upon the redox processes decreased as the dendrimer generation decreased. This made the changes in frequency due to the anion exchange more clearly defined. Figure 4 shows A) the typical cyclic voltammetric and B) frequency responses for a Pt electrode on a quartz-crystal resonator in contact with a 0.2 mM solution of dendrimer **1**. As can be seen in the cyclic voltammogram, both the cathodic and anodic waves showed a diffusional shape, unlike the stripping shape observed for **4**; this suggests that, apparently, no electrodeposition takes place. In addition, the frequency

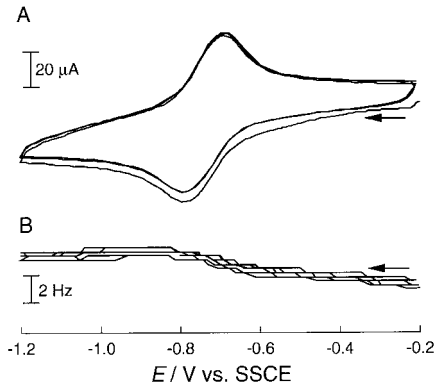

Figure 4. Typical A) current (CV) and B) frequency responses as a function of applied potential at 50 mV s^{-1} for a Pt EQCM electrode in contact with a solution of dendrimer **1** (50 μM; 0.2 mM cobaltocenium sites).

response appeared to be a simpler anion-exchange type. However, there was a slight decrease in frequency from about -1.0 V versus SSCE in the cathodic scan, and a slight increase in the anodic scan up to about -1.0 V. These frequency changes could be a manifestation of a slight accumulation and desorption of the dendrimer upon reduction and oxidation, respectively, similar to those observed in the case of **4**. The magnitude of this decrease in the frequency (accumulation of the dendrimer) upon reduction increased for the larger generations as would be anticipated, since a larger dendrimer should have lower solubility.

A cyclic voltammogram and frequency response for **2** are depicted in Figures 5A and 5B, respectively. As can be seen, the anodic peak of the cyclic voltammogram is sharper than

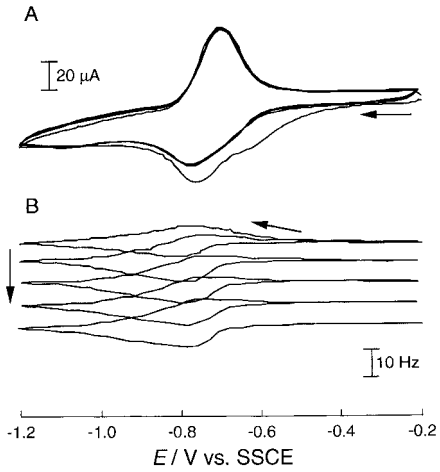

Figure 5. Typical A) current (CV) and B) frequency responses as a function of applied potential at 50 mV s^{-1} for a Pt EQCM electrode in contact with a solution of dendrimer **2** (25 μM; 0.2 mM cobaltocenium sites) in TBAH/CH_3CN (0.10 M).

that of **1**, indicating that the dendrimer accumulated on the electrode surface in the cathodic potential scan. The frequency change appeared to have contributions from both the anion exchange and the dendrimer deposition/desorption processes. Unlike **4**, the overall frequency decreased upon continuous potential cycling, suggesting that some of the dendrimer remained on the electrode even upon oxidation. This would suggest a slower rate of desorption of the deposited **2** relative to **4**. When the potential was held at -0.2 V, at which the dendrimer is in its oxidized form, there was a partial desorption of the dendrimer so that the frequency gradually increased until it reached a steady state value that was several Hz lower than the initial one prior to adsorption of the dendrimer. This again suggests that there is some adsorption of the dendrimer prior to electroreduction. Assuming that the entire frequency change was due to adsorbed dendrimer, we estimate the coverage is close to a monolayer. The slower desorption of **2** might be due to a smaller number of positive charges ($+8$) in its oxidized form and a resulting smaller electrostatic repulsion compared with **4** ($+32$). The cyclic voltammetric and frequency responses for **3** appeared to be intermediate between those exhibited by **4** and **2**.

Changes in film morphology were studied by using admittance measurements of the quartz-crystal resonator on the basis of its electrical equivalent circuit, especially in terms of its resistance parameter. Theoretical aspects of admittance measurements (resistance parameter) have been described previously.[25] Figure 6 shows changes of the resistance param-

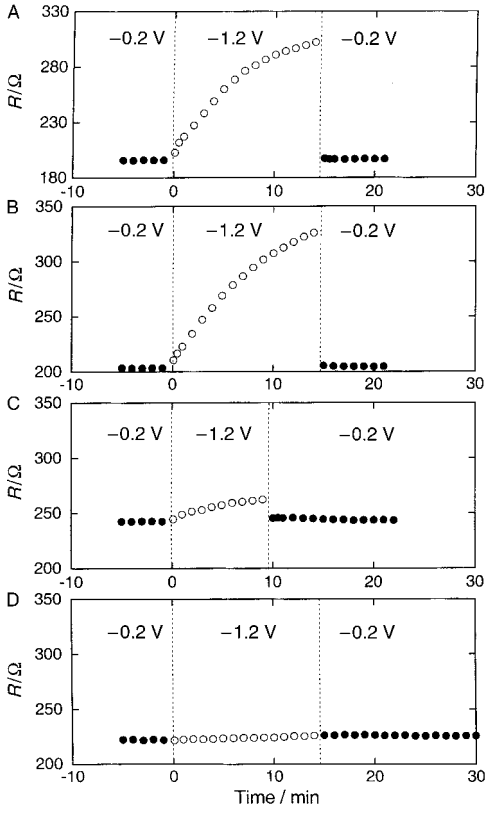

Figure 6. Time-courses of the resistance parameter of a quartz-crystal resonator during potential step experiments (between -0.20 V and -1.20 V versus SSCE) in a solution of A) **4**, B) **3**, C) **2**, and D) **1** (0.2 mM cobaltocenium sites) in TBAH/CH_3CN (0.10 M) .

eter for the equivalent circuit of the resonator versus time in a 0.1 M TBAH/CH_3CN solution containing 0.2 mM cobaltocenium sites of dendrimers **1**–**4** at applied potentials of -0.20 and -1.20 V versus SSCE, at which the charge on each metal center is $+1$ and 0, respectively. As can be seen in Figures 6A

0947-6539/01/0705-1114 $ 17.50+.50/0 *Chem. Eur. J.* **2001**, *7*, No. 5

and 6B, the resistance sharply increased upon potential stepping from -0.20 and -1.20 V for both **4** and **3**. The resistance rapidly decreased to the original value when the potential was stepped back to -0.20 V. These increases in resistance are believed to arise from an increase in the thickness, roughness, and viscoelasticity of the film due to the continuous accumulation of the dendrimers at -1.20 V. On the other hand, the decreases in the resistance are believed to arise from the dissolution of the dendrimer from the electrode. These observations are opposite to those of the analogous ferrocenyl dendrimers for which the resistance increased upon oxidation of the dendrimer and decreased upon reduction. In contrast, in the case of **1** (Figure 6D) the resistance remained nearly constant, indicating that there were no significant accumulation and, thus no morphological changes upon reduction. Changes in the resistance parameter for **2** appeared to be intermediate between those exhibited by **1** and **3**. These results are in agreement with the frequency changes mentioned previously.

Atomic force microscopy (AFM) imaging:In an effort to better characterize the structure of adsorbed layers of these cobaltocenium dendrimers, we have carried out tapping-mode AFM (TMAFM) studies in air (ex situ). We followed the same general procedures employed in our previous work[14b] on the related ferrocenyl dendrimers. In that case, and by using noncontact (i.e., tapping mode) AFM, we were able to image, down to the molecular level, films derived from DAB-*dend*-Fc_{64}. The observation of single dendrimer molecules by contact mode AFM (CMAFM) in air was not possible owing to the strong effect of the tip on the film, dragging the dendrimers upon scanning.

Figure 7A shows an AFM image (in air) of a freshly annealed Pt(111) electrode where the image, as expected, is essentially featureless. The surface was subsequently modified with a film of **4** as described in the experimental section and again imaged by TMAFM. A representative image is presented in Figure 7B; this shows clear evidence of the presence of adsorbed dendrimers. The circular features that can be seen over the entire image represent individual dendrimer units. Also from the figure, it is evident that in some cases there appear to be aggregates present on the surface. We ascribe these brighter spots to the presence of adsorbates that are two dendrimer units in height. A preliminary analysis of such images suggests that the apparent size (7.8 ± 1.0 nm) of the adsorbed dendrimer is larger than the calculated (4.4 nm diameter for **4**) value. The difference in size can be attributed mainly to two factors: flattening of the dendrimers upon adsorption and the effect commonly known as "convolution", whereby the image obtained is composed of the imaged feature and a "reflection" of the tip geometry. The flattening of dendrimer molecules upon adsorption is an effect we[14b] as well as Crooks and co-workers[26] have previously documented and is, in fact, an effect common to "soft" adsorbates. The second effect is inherent to scanning probe microscopies and constitutes a significant problem for particle analysis, especially in cases where the tip geometry is unknown and the features imaged are of size comparable to the tip dimensions (radius). There are also strong tip effects

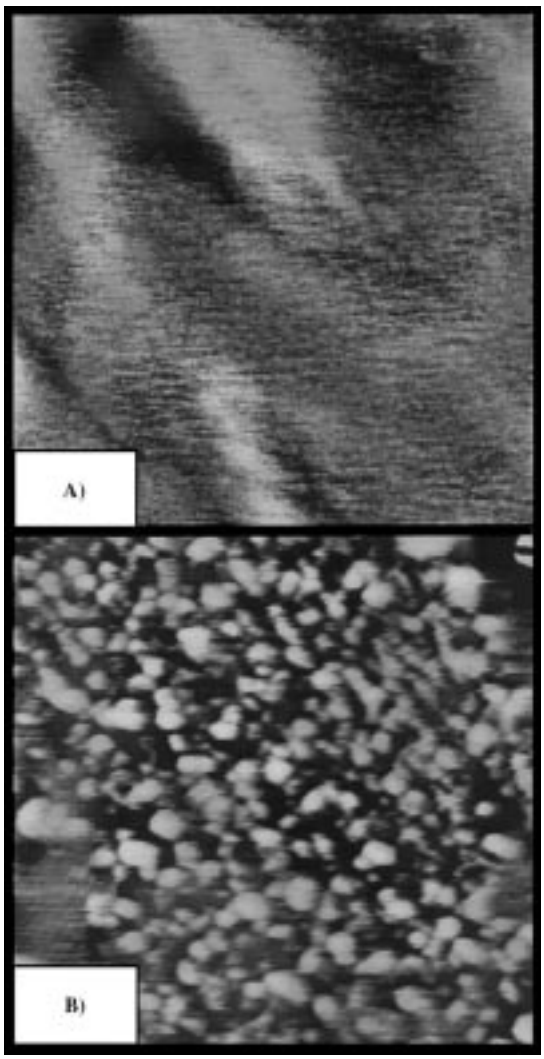

Figure 7. A) AFM image of freshly annealed Pt(111) single crystal. B) TMAFM of the same Pt(111) crystal modified with metallodendrimer **4**. Both images are 200×200 nm.

that can drag adsorbates, indent soft surfaces, and limit the ability to obtain molecularly resolved images. Tip effects on adsorbed films imaged in air are often caused by a capillary layer of water formed between the surface and the tip. Imaging in a solvent usually eliminates this effect, although many samples are softer when solvated. In addition to these ex situ studies in air, we are currently carrying out electrochemical AFM (ECAFM) studies in situ and results from these investigations will be presented elsewhere.

Conclusion

Multimetallic diaminobutane-based poly(propylene imine) dendrimers that contain 4, 8, 16, and 32 peripheral cobaltocenium units (**1**–**4**) have been synthesized and characterized.

The redox activity of the cobaltocenium centers in **1**–**4** has been characterized by means of CV and the electrochemical quartz-crystal microbalance. All of the dendrimers exhibit reversible redox chemistry associated with the cobaltocenium/cobaltocene redox couple, whose formal potential E° is shifted positively (relative to the cobaltocenium/cobaltocene

redox couple in the same medium) due to the strong electron-withdrawing effect of the amide groups within the dendrimer backbone. Upon reduction, the dendrimers exhibit a tendency to electrodeposit onto the electrode surface, which is more pronounced for the higher generations. Pt and glassy carbon electrodes could be modified with films derived from **1**–**4** exhibiting a well-defined and persistent electrochemical response. EQCM measurements show that the dendrimers adsorb, at open circuit, onto Pt surfaces at monolayer or submonolayer coverage. Potential scanning past -0.75 V, at which the cobaltocenium sites are reduced, gave rise to the electrodeposition of multilayer equivalents of the dendrimers, likely due to decreased solubility of the neutral dendrimer. The additional material gradually desorbs upon re-oxidation so that only a monolayer equivalent remains on the electrode surface. Changes in film morphology as a function of dendrimer generation and surface coverage were studied by means of admittance measurements of the quartz-crystal resonator on the basis of its electrical equivalent circuit, especially in terms of its resistance parameter. In general we find that films of the lower dendrimer generation **1** behave rigidly, whereas those of the higher generation **4** exhibit viscoelastic behavior with intermediate behavior being exhibited by films of **2** and **3**. Using tapping mode AFM, we have been able to obtain molecularly resolved images of **4** adsorbed on a Pt(111) electrode.

Experimental Section

General: All reactions were performed under an inert atmosphere (prepurified N_2 or Ar) using standard Schlenk techniques. Solvents were dried by standard procedures over the appropriate drying agents and distilled immediately prior to use. Triethylamine (Merck) was distilled over KOH under N_2. The hexafluorophosphate salt of 1-(chlorocarbonyl)cobaltocenium was prepared as described in the literature[27] by treatment of carboxycobaltocenium hexafluorophosphate with an excess of freshly distilled $SOCl_2$. The excess $SOCl_2$ was removed under vacuum, and the resulting yellow solid was thoroughly washed with hexane and dried under vacuum. The dendritic polyamines DAB-*dend*-$(NH_2)_x$ ($x = 4$, 8, 16, and 32) were purchased from DSM. Sephadex LH-20 (Fluka) was used for column chromatographic purifications. NMR spectra were recorded on a Bruker AMX (^{1}H, 300 MHz; ^{13}C, 75.43 MHz) spectrometer. Infrared spectra were recorded on a Bomem MB-100 FTIR spectrometer. ESI-MS was carried out with a Hewlett Packard quadrupole mass spectrometer, model 1100 coupled to an HPLC system. The samples were introduced into the source by constant infusion or direct injection (FIA). FAB mass spectral analyses were conducted on a VG Auto Spec mass spectrometer equipped with a cesium ion gun.

Electrochemical measurements: Cyclic voltammetric experiments were performed on a BAS CV-27 potentiostat. Electrochemical measurements were performed in CH_3CN freshly distilled from calcium hydride under nitrogen. The supporting electrolyte was in all cases tetra-*n*-butylammonium hexafluorophosphate (TBAH, Aldrich), which was purified by recrystallization from ethanol and dried under vacuum; it was used in a concentration of 0.10 M in all cyclic voltammetric measurements. A conventional sample cell operating under an atmosphere of prepurified nitrogen was used for CV. All cyclic voltammetric experiments were performed with either a Pt-disk working electrode ($A = 0.02$ cm^2) or a glassy carbon-disk working electrode ($A = 0.070$ cm^2), each of which was polished prior to use with either 1 μm diamond paste (Buehler) or 0.05 mm alumina/water slurry and rinsed thoroughly with purified water and acetone. Potentials are referenced to a saturated calomel electrode (SCE) without regards to the liquid junction potential. A large area-coiled Pt wire was used as a counter electrode. No *iR* compensation was used. The modification of electrode surfaces (Pt or glassy carbon electrodes) was effected by continuous scanning between 0 and -1.10 V versus SCE, in degassed solutions of the dendrimer in CH_3CN. The electrodes thus coated were rinsed with CH_3CN to remove any adhering solution and dried in air. NPV measurements were performed on a Autolab-PGSTAT 12 potentiostat using a Pt-disk working electrode ($A = 0.02$ cm^2), at a scan rate of 10 mV s^{-1}.

EQCM measurements: The EQCM apparatus and instrumentation for the resistance parameter measurements of a resonator have been previously described.[14b] AT-cut quartz crystals (5 MHz) of 24.5 mm diameter with Pt electrodes deposited over a Ti adhesion layer (Maxtek Co.) were used for EQCM measurements. An asymmetric keyhole electrode arrangement was used, in which the circular electrode geometrical areas were 1.370 cm^2 (front side) and 0.317 cm^2 (back side). The electrode surfaces were overtone polished. The quartz-crystal resonator was set in a probe (TPS-550, Maxtek) made of Teflon®, in which the oscillator circuit was included, and the quartz crystal was held vertically. The probe was connected to a conventional three-chamber electrochemical cell by a home made Teflon® joint. One of the electrodes of the quartz-crystal resonator, in contact with the solution, was also used as the working electrode. The potential of the working electrode was controlled with a potentiostat (CV-27, BAS). A sodium chloride saturated calomel electrode (SSCE) and a coiled Pt wire were used as reference and counter electrodes, respectively. The frequency response measured with a plating monitor (PM-740, Maxtek) and the current measured with the potentiostat were simultaneously recorded by a personal computer, which was interfaced to the above instruments. The admittance of the quartz-crystal resonator was measured near its resonant frequency by an impedance analyzer (HP4194A, Hewlett-Packard) equipped with a test lead (HP16048A). A probe similar to the one used in the EQCM measurements, but which did not include an oscillator circuit inside, was used to accomplish a direct connection of the quartz-crystal resonator to the impedance analyzer.

AFM measurements: TMAFM studies were carried out on a Nanoscope III (Digital Instruments) microscope, with a 12 μm D scanner in air. The AFM was mounted on a home-made antivibration table and on an isolation chamber. All images shown are unfiltered and taken online; no offline zoom was used.

The modified Pt samples for TMAFM analysis were prepared by immersion of the freshly flame-annealed Pt single crystal in a 0.25 μM solution of **4** in CH_3CN solution for 2 h. The electrode was subsequently washed with fresh CH_3CN and air dried before TMAFM analysis.

Tapping-mode analysis was carried out at different size ranges from nm to μm at various locations on the surface prior to and after modification with **4**. All data were recorded in height mode. Set point values were chosen so that the interaction of the tip and the sample gave rise to a good compromise between stability and resolution, without destroying the tip or the sample. Scan rates ranged from 1 to 3 Hz to avoid deformation of the image. At higher scan rates several problems arose ranging from damage of the tip to distortion of the image due to a slow vertical response for the surface profile. Images were taken at a 512×512 pixel resolution to increase the detail in the images.

Syntheses of cobaltocenium dendrimers: All dendrimers were prepared following the same procedure. A solution of the dendritic polyamine DAB-*dend*-$(NH_2)_x$ ($x = 4$, 8, 16, 32) and triethylamine in dry CH_3CN was added dropwise to a stirred solution of 1-(chlorocarbonyl)cobaltocenium hexafluorophosphate (10% excess) in CH_3CN under argon at room temperature. The reaction mixture was stirred overnight. The resulting greenish mixture was filtered, the solvent was removed under vacuum, and the residue was dissolved in CH_3CN and precipitated into CH_2Cl_2 to remove the triethylammonium chloride byproduct. The precipitate was purified by column chromatography on Sephadex LH-20 with CH_3CN as eluent. The first yellow or greenish band containing the corresponding cobaltocenium dendrimer was separated, and after drying under vacuum the dendrimers were isolated as yellow, orange, and greenish shiny solids. Yields were in the 30–60% range.

Selected characterization data for dendrimer 1: ^{1}H NMR ($(CD_3)_2CO$): $\delta =$ 8.24 (t, 4H; N*H*), 6.34 (t, 8H; C_5H_4), 5.98 (t, 8H; C_5H_4), 5.92 (s, 20H; Cp), 3.52 (quartet, 8H; NHCH_2), 3.06 (br, 12H; CH_2NCH_2), 2.07 (br, 8H; $CH_2CH_2CH_2$), 1.86 (br, 4H; $NCH_2CH_2CH_2CH_2N$); ^{13}C{^{1}H} NMR ([D$_6$]DMSO): $\delta = 161.54$ (*C*O), 94.00, 85.84, 83.98 (C_5H_4), 86.03 (Cp),

0947-6539/01/0705-1116 $ 17.50+.50/0 *Chem. Eur. J.* **2001**, *7*, No. 5

52.42 and 50.60 (CH_2NCH_2), 37.44 (NH-CH_2), 24.92 and 22.67 ($CH_2CH_2CH_2$); IR (KBr): $\tilde{\nu}$ = 1662 (amide I), 1545 cm^{-1} (amide II); MS (FAB): *m/z* (%): 1758 (38) $[M+H]^+$, 1611 (100) $[M-PF_6]^+$, 1466.4 (61) $[M-2PF_6]^+$, 1321 (18) $[M-3PF_6]^+$, 734 (30) $[M-2PF_6]^{2+}$.

Selected characterization data for dendrimer 2: ^1H NMR ($(CD_3)_2CO$): δ = 8.69 (br, 8H; N*H*), 6.45 (t, 16H; C_5H_4), 5.97 (t, 16H; C_5H_4), 5.94 (s, 40H; Cp), 3.53 (br, 16H; $NHCH_2$), 3.33, 3.02 (br, 36H; CH_2NCH_2), 2.18 (br, 28H; CH_2CH_2N), 1.82 (br, 4H; $NCH_2CH_2CH_2CH_2N$); $^{13}C\{^1H\}$ NMR ([D_6]DMSO): δ = 161.59 (*C*O), 93.87, 85.82, 84.11 (C_5H_4), 86.06 (Cp), 50.43 (CH_2NCH_2), 37.29 (NH-CH_2), 24.24 ($CH_2CH_2CH_2$); IR (KBr): $\tilde{\nu}$ = 1663 (amide I), 1550 cm^{-1} (amide II); MS (FAB): *m/z* (%): 3655 (72) $[M+H]^+$, 3509 (100) $[M-PF_6]^+$, 3364 (95) $[M-2PF_6]^+$, 3218 (42) $[M-3PF_6]^+$, 3074 (41) $[M-4PF_6]^+$, 1681.8 $[M-2PF_6]^{2+}$.

Selected characterization data for dendrimer 3: ^1H NMR ([D_6]DMSO): δ = 8.97 (br, 16H; N*H*), 6.26 (br, 32H; C_5H_4), 5.88 (br, 32H; C_5H_4), 5.81 (s, 80H; Cp), 3.29 (br, 32H; $NHCH_2$), 2.96, 2.65 (br, 84H; CH_2NCH_2), 1.88 (br, 56H; $CH_2CH_2CH_2$), 1.68 (br, 4H; $NCH_2CH_2CH_2CH_2N$); $^{13}C\{^1H\}$ NMR ([D_6]DMSO): δ = 161.37 (*C*O), 93.55, 85.59, 83.80 (C_5H_4), 85.78 (Cp), 50.04, 49.45 (CH_2NCH_2), 36.95 (NH-CH_2), 23.84, 20.34 ($CH_2CH_2CH_2$); IR (KBr): $\tilde{\nu}$ = 1662 (amide I), 1552 cm^{-1} (amide II); MS (electrospray): *m/z*: 1096 $[M-6PF_6]^{6+}$, 919 $[M-7PF_6]^{7+}$, 786 $[M-8PF_6]^{8+}$, 683 $[M-9PF_6]^{9+}$, 600 $[M-10PF_6]^{10+}$, 532 $[M-11PF_6]^{11+}$, 476 $[M-12PF_6]^{12+}$.

Selected characterization data for dendrimer 4: ^1H NMR ([D_6]DMSO): δ = 9.14 (br, 32H; N*H*), 6.33 (br, 64H; C_5H_4), 5.89 (br, 64H; C_5H_4), 5.83 (s, 160H; Cp), 3.31 (br, 64H; $NHCH_2$), 3.09–2.74 (br, 180H; CH_2NCH_2), 1.92 (br, 64H; $CH_2CH_2CH_2$); $^{13}C\{^1H\}$ NMR ([D_6]DMSO): δ = 162.29 (*C*O), 94.50, 86.56, 84.90 (C_5H_4), 86.80 (Cp), 51.13, 50.35 (CH_2NCH_2), 37.95 (NH-CH_2), 24.70, 21.21 ($CH_2CH_2CH_2$); IR (KBr): $\tilde{\nu}$ = 1667 (amide I), 1561 cm^{-1} (amide II).

Acknowledgement

This work was supported by the Office of Naval Research and the Cornell Center for Materials Research (CCMR), and by the Spanish Dirección General de Enseñanza Superior e Investigación Científica (PB-97–0001). DJD acknowledges support by a R. Sproull Fellowship from CCMR and a Ford predoctoral fellowship. HDA acknowledges support through the Profesores Visitantes Iberdrola program.

[1] For reviews, see for example: a) G. R. Newkome, C. N. Moorefield, F. Vögtle, *Dendritic Molecules: Concepts, Synthesis, Perspectives*, VCH, Weinheim, **1996**; b) M. Fischer, F. Vögtle, *Angew. Chem.* **1999**, *111*, 934; *Angew. Chem. Int. Ed.* **1999**, *38*, 884; c) D. A. Tomalia, H. D. Durst, *Top. Curr. Chem.* **1993**, *165*, 193; d) J. M. J. Fréchet, *Science* **1994**, *263*, 1710; e) N. Ardoin, D. Astruc, *Bull. Soc. Chim. Fr.* **1995**, *132*, 875; f) A. W. Bosman, H. M. Janssen, E. W. Meijer, *Chem. Rev.* **1999**, *99*, 1665; g) J.-P. Majoral, A.-M. Caminade, *Chem Rev.* **1999**, *99*, 845; h) H. F. Chow, T. K. K. Mong, M. F. Nongrum, C. W. Wan, *Tetrahedron* **1998**, *54*, 8543.

[2] G. R. Newkome, E. He, C. N. Moorefield, *Chem. Rev.* **1999**, 1689.

[3] M. Hearshaw, J. R. Moss, *Chem. Commun.* **1999**, 1.

[4] M. Venturi, S. Serroni, A. Juris, S. Campagna, V. Balzani, *Top. Curr. Chem.* **1998**, *197*, 193.

[5] I. Cuadrado, M. Morán, C. M. Casado, B. Alonso, J. Losada, *Coord. Chem. Rev.* **1999**, *193–195*, 395.

[6] C. Gorman, *Adv. Mater*. **1998**, *10*, 295.

[7] F. J. Stoddart, T. Welton, *Polyhedron* **1999**, *18*, 3575.

[8] a) B. Alonso, I. Cuadrado, M. Morán, J. Losada, *J. Chem. Soc. Chem. Commun.* **1994**, 2575; b) C. M. Casado, I. Cuadrado, M. Morán, B. Alonso, M. Barranco, J. Losada, *Appl. Organomet. Chem.* **1999**, *13*, 245; c) I. Cuadrado, M. Morán, C. M. Casado, B. Alonso, F. Lobete, B. García, M. Ibisate, J. Losada, *Organometallics* **1996**, *15*, 5278.

[9] I. Cuadrado, C. M. Casado, B. Alonso, M. Morán, J. Losada, V. Belsky, *J. Am. Chem. Soc.* **1997**, *119*, 7613.

[10] a) C. Valerio, J.-L. Fillaut, J. Ruiz, J. Guittard. J.-C. Blais, D. Astruc, *J. Am. Chem. Soc.* **1997**, *119*, 2588; b) S. Nlate, J. Ruiz, J.-C. Blais, D. Astruc, *Chem. Commun.* **2000**, 417.

[11] a) Y. Wang, C. M. Cardona, A. E. Kaifer, *J. Am. Chem. Soc.* **1999**, *121*, 9756; b) C. M. Cardona, A. E. Kaifer, *J. Am. Chem. Soc.* **1998**, *120*, 4023.

[12] C.-F. Shu, H.-M. Shen, *J. Mater. Chem.* **1997**, *7*, 47.

[13] S. Achar, C. E. Immoos, M. G. Hill, V. J. Catalano, *Inorg. Chem.* **1997**, *36*, 2314.

[14] a) B. Alonso, M. Morán, C. M. Casado, F. Lobete, J. Losada, I. Cuadrado, *Chem. Mater.* **1995**, *7*, 1440; b) K. Takada, D. J. Díaz, H. Abruña, I. Cuadrado, C. M. Casado, B. Alonso, M. Morán, J. Losada, *J. Am. Chem. Soc.* **1997**, *119*, 10763.

[15] a) C. M. Casado, B. González, I. Cuadrado, B. Alonso, M. Morán, J. Losada, *Angew. Chem.* **2000**, *112*, 2219; *Angew. Chem. Int. Ed.* **2000**, *39*, 2135; b) J. Losada, I. Cuadrado, M. Morán, C. M. Casado, B. Alonso, M. Barranco, *Anal. Chim. Acta* 1996, *251*, 5.

[16] R. Castro, I. Cuadrado, B. Alonso, C. M. Casado, M. Morán, A. Kaifer, *J. Am. Chem. Soc.* **1997**, *119*, 5760.

[17] C. M. Casado, I. Cuadrado, B. Alonso, M. Morán, J. Losada, *J. Electroanal. Chem.* **1999**, *463*, 87.

[18] a) C. Valerio, E. Alonso, J. Ruiz, J.-C. Blais, D. Astruc, *Angew. Chem.* **1999**, *111*, 1855; *Angew. Chem. Int. Ed.* **1999**, *38*, 1747; b) F. Moulines, L. Djakovitch, R. Boese, B. Gloaguen, W. Thiel, J.-L. Fillaut, M.-H. Delville, D. Astruc, *Angew. Chem.* **1993**, *101*, 1132; *Angew. Chem. Int. Ed. Engl.* **1993**, *38*, 1075; c) E. Alonso, C. Valerio, J. Ruiz, D. Astruc, *New J. Chem.* **1997**, *21*, 1139.

[19] B. González, C. M. Casado, B. Alonso, I. Cuadrado, M. Morán, Y. Wang, A. E. Kaifer, *Chem. Commun.* **1998**, 2569.

[20] A. J. Bard, L. R. Faulkner, *Electrochemical Methods*, Wiley, New York, **1980**, Chapter 5.

[21] D. Albagli, G. Bazan, M. S. Wrighton, R. R. Schrock, *J. Am. Chem. Soc.* **1992**, *114*, 4150.

[22] J. I. Goldsmith, H. D. Abruña, unpublished results.

[23] a) "Electrode Modification with Polymeric Reagents", H. D. Abruña in *Electroresponsive Molecular and Polymeric Systems*, *Vol. 1* (Ed.: T. A. Skotheim), Dekker, New York, NY, **1988**; b) R. W. Murray in *Molecular Design of Electrode Surfaces, Techniques of Chemistry XXII* (Ed.: R. W. Murray), Wiley, New York, NY, **1992**, p. 1.

[24] a) G. D. Storrier, K. Takada, H. D. Abruña, *Langmuir* **1999**, *15*, 872; b) K. Takada, G. D. Storrier, M. Morán, H. D. Abruña, *Langmuir* **1999**, *15*, 7333.

[25] a) R. Beck, U. Pittermann, K. G. Weil, *Ber. Bunsenges. Phys. Chem.* **1988**, *92*, 1363; b) S. Martin, V. E. Granstaff, G. Frye, *Anal. Chem.* **1991**, *63*, 2272; c) M. Yang, M. Thompson, *Anal. Chem.* **1993**, *65*, 1158; d) D. A. Buttry, M. D. Ward, *Chem. Rev.* **1992**, *92*, 1355.

[26] a) A. Hierlemann, J. K. Campbell, L. A. Baker, R. M. Crooks, A. J. Ricco, *J. Am. Chem. Soc.* **1998**, *120*, 5323; b) M. Wells, R. M. Crooks, *J. Am. Chem. Soc.* **1996**, *118*, 3988.

[27] J. E. Sheats, M. D. Rausch, *J. Org. Chem.* **1970**, *35*, 3254.

Received: July 26, 2000 [F2626]